USE OF THE AZIMUTH WAVELENGTH CUT-OFF TO RETRIEVE THE SEA SURFACE WIND SPEED FROM SENTINEL 1 AND COSMO-SKYMED SAR DATA

G. Grieco [(1)], F. Nirchio[(1)], A. Montuori [(2)], M. Migliaccio[(3)] , W. Lin [(4)], M. Portabella[(4)]

[(1)]Agenzia Spaziale Italiana, Contrada Terlecchia, Matera, Italy, giuseppe.grieco@est.asi.it
[(1)]Agenzia Spaziale Italiana, Contrada Terlecchia, Matera, Italy, Francesco.nirchio@asi.it
[(2)] Istituto Nazionale di Geofisica e Vulcanologia, Centro Nazionale Terremoti, Rende, Italy, antonio.montuori@ingv.it
[(3)]Università degli Studi di Napoli Parthenope, Centro direzionale Isola C4, Napoli, Italy, migliaccio@uniparthenope.it
[(4)] Institute de Ciències del Mar (ICM-CSIC), Passeig Marítim de la Barceloneta 37-49, Barcelona, Spain, wenminglin@icm.csic.es

[(4)] Institute de Ciències del Mar (ICM-CSIC), Passeig Marítim de la Barceloneta 37-49, Barcelona, Spain, portabella@icm.csic.es

ABSTRACT

The dependency of the azimuth wavelength cut-off on the wind speed has been studied through a dataset of Sentinel-1 multi look SAR images co-located with wind speed measurements, significant wave height and mean wave direction from ECMWF operational output.
A Geophysical Model Function (GMF) has been fitted and a retrieval exercise has been done comparing the results to a set of independent wind speed scatterometer measurements of the Chinese mission HY-2A. The preliminary results show that the dependency of the azimuth cut-off on the wind speed is linear only for fully developed sea states and that the agreement between the retrieved values and the measurements is good especially for high wind speed.
A similar approach has been used to assess the dependency of the azimuth cut-off also for X-band COSMO-SkyMed data. The dataset is still incomplete but the preliminary results show a similar trend.

1. INTRODUCTION

Sea wind estimation by Synthetic Aperture Radar (SAR) measurements is a topic of relevance both on the scientific and user side. There exist several empirical approaches in order to retrieve the sea wind field from SAR images ([3], [5]), but more has still to be done.
The azimuth wavelength cut-off (λ_C) is a measure of the well-know distortive non-linear effect that occurs during the SAR imaging process of a moving target surface such as the ocean. λ_C has at least two contributions: 1) the velocity bunching imaging mechanism [2] and 2) the intrinsic scene coherence time due to the finite lifetime of scatterers [7].
Under the hypothesis of linear waves, λ_C is expressed as follows [4]:

$$\lambda_C = \pi \frac{R}{V} \sqrt{\int_0^\infty \omega^2 S(\omega) F(\omega, \theta, \phi)} \qquad (1)$$

where R is the range to target, V is the platform velocity, ω is the angular frequency, S is the intensity of the ω-component of the wave spectrum, F takes into account the directionality aspects of the sea wave spectrum and ϕ is the relative direction of the ω-component to the range direction.
The λ_C approach for the wind speed (U) retrieval is not new. It dates back at least to 1998 [4]. In this paper, the authors show that the dependency of λ_C on U is roughly linear. Anyway, the linear trend can be considerably altered by the presence of swell and the sea age plays a key role. Furthermore, they remark the dependency of λ_C on the incidence angle (θ) and on the directionality of the sea wave spectrum (eq. 1). When dealing with λ_C relating to SAR images acquired at different θ one should produce a "normalization" that takes into accounts its dependency on both θ and ϕ.
The λ_C approach should be considered as a potential complementary tool to the already existing Geophysical Model Functions (GMFs). Furthermore, the computation of λ_C does not need any calibrated Normalized Radar Cross Section (NRCS), therefore a λ_C-GMF can potentially be used to retrieve U from every SAR platform, given that the necessary normalization for the different acquisition geometries is produced.
In this paper, the dependency of λ_C on U is assessed in view of the new Sentinel-1 (S-1) data. These data are co-located with U, significant wave height (H_S) and mean wave direction (MWD) from ECMWF operational output. A λ_C-GMF is fitted and then validated through an independent dataset of S-1 images co-located with scatterometer wind measurements of the Chinese mission HY-2A.
Finally, the dependency of λ_C on U is assessed also through a dataset of X-band SAR images of the COSMO-SkyMed mission co-located with ECMWF operational output and scatterometer wind measurements of the QuickScat mission. This dataset needs to be expanded in order to better reproduce all the possible sea/wind situations.

Proc. 'Living Planet Symposium 2016', Prague, Czech Republic, 9–13 May 2016 (ESA SP-740, August 2016)

2. DATASET

The training dataset consists of 355 S-1 multi look images acquired at θ varying from 20° to 45°. The images are co-located with U, H_S and MWD from ECMWF operational output. All SAR images have been acquired over the Hawaiian archipelago and on the northeast Atlantic Ocean since the beginning of November 2014 to the end of April 2015. The total number of samples is 5355, 1065 of which are in fully developed sea state.

The validation dataset consists of 99 independent SAR images acquired over the same area and on the same period of the training dataset. These images are co-located with scatterometer wind measurements of the Chinese mission HY-2A (HSCAT) and with H_S and MWD from ECMWF operational output. The total number of samples in fully developed sea is 187.

The COSMO-SkyMed dataset consists of 80 multi look SAR images acquired over the equatorial Atlantic Ocean, from July to November 2009 with θ in the range from 20° to 45°. These images are co-located with scatterometer wind measurements of the QuickScat mission and with H_S and MWD from ECMWF operational output. The total number of samples is 128, 40 of which are in fully developed sea.

3. METHODOLOGY

The λ_C-GMF is linear and its coefficients are fitted through a least square regression. The model is written as follows:

$$\lambda_C = a + bU \qquad (2)$$

The model is fitted only for fully developed sea states. Such situations are identified through the Pierson-Moskowitz spectrum [6], where H_S is related to U through the following equation:

$$H_S^{FD} = 0.22\frac{U^2}{g} \qquad (3)$$

g being the gravity constant. Before fitting the model, λ_C is normalized through the following equation:

$$\lambda_C^* = \frac{R(\theta = 20°)\sqrt{F(\theta = 20°, \phi_0 = 0°)}\lambda_C}{R(\theta)\sqrt{F(\theta, \phi_0)}} \qquad (4)$$

where ϕ_0 is the relative MWD to the range direction and F comes from [4]:

$$F = \cos^2(\theta) + \sin^2(\theta)\left[\frac{1}{2} + \frac{1}{4}\cos(2\phi_0)\right] \qquad (5)$$

In other words, λ_C^* is the azimuth cut-off that we should expect if the SAR image was acquired at θ=20° and ϕ_0=0°. Furthermore, we suppose that the directionality spectrum could be represented by the MWD only. This is a rough approximation and a refinement should be produced in the future.

4. RESULTS

Fig. 1 shows the scatter plot of normalized λ_C^* (here on simply λ_C) versus U. The marker size is proportional to H_S while the maker colour represents the difference between H_S and $H^{FD}{}_S$. It can be seen that the larger the marker, the higher λ_C. This result is not new and therefore quite expected [1]. Furthermore, it can be seen that the red markers are mainly located in the upper left part of the upper side scatter plot, where U is not higher than 10 ms^{-1} and λ_C is higher than 300 m. For such cases, H_S is much higher than it would be in case of fully developed sea. In other words, such situations are representative of swell. Blue markers are representative of the opposite case: H_S is much lower that we should expect in fully developed sea. Light blue markers are representative of fully developed sea cases.

We can conclude that λ_C has a clear dependency on U, but the dependency on the sea age is not negligible, in agreement with what stated in [4]. If we focus our attention on fully developed sea situations (bottom side plot), the correlation between λ_C and U increases (r from 0.62 to 0.76) and the trend is roughly linear. Therefore, we conclude that an azimuth cut-off approach for the retrieval of U can be pursued only in case of fully developed sea.

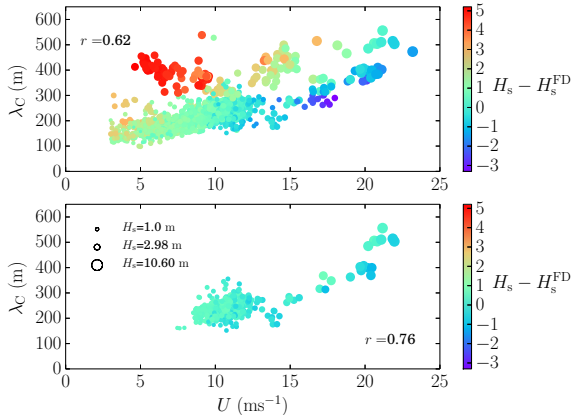

Figure 1: Scatter plot of λ_C versus U. The upper side plot considers all the samples while the bottom side one refers to fully developed sea state only. The marker size is proportional to the significant wave height (H_S), while the colour is proportional to the difference between H_S and $H^{FD}{}_S$. Red markers are representative of swell, while blue markers are representative of growing sea. Light blue markers are representative of fully developed sea cases. r is the correlation coefficient.

Fig. 2 shows the retrieval of U versus the scatterometer measurements.

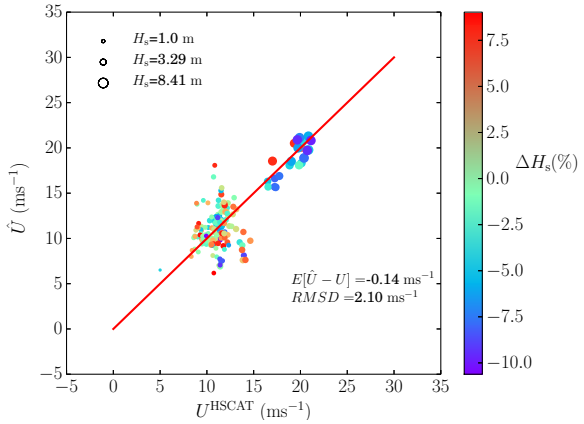

Figure 2: Scatter plot of retrieved U versus scatterometer measurements. The marker size is proportional H_S to while the maker colour is representative of the difference between H_S and $H^{FD}{}_S$. E[] is the bias and RMSD is the Root Mean Square Difference.

First of all, it can be seen that there is only one sample with U lower than 8 ms^{-1}, therefore this validation exercise is not representative of all the possible wind speed situations. On the other side, a non-negligible number of samples is representative of high U cases. Furthermore, we can see that all the markers roughly follow the diagonal. In particular, high U are much better retrieved with respect to medium range U.
Finally, Fig. 3 shows two scatter plots for the COMOS-SkyMed (CSK) dataset.

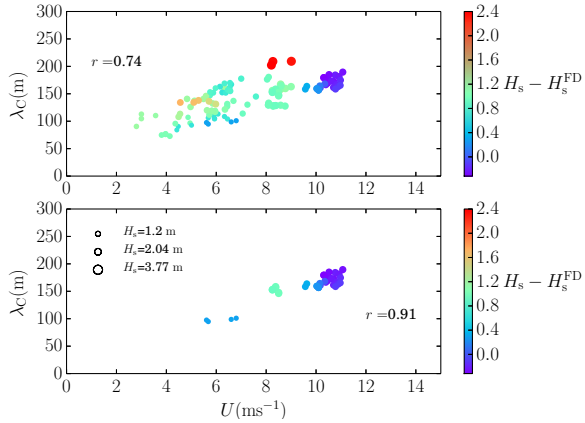

Figure 3: Scatter plot of λ_C versus U. The upper side plot shows all samples while the bottom side one refers to fully developed sea state cases only. The marker size is proportional to the significant wave height (H_S), while the colour is proportional to the difference between H_S and $H^{FD}{}_S$. r is the correlation coefficient.

This analysis is at a very preliminary stage. Indeed, it can be seen that the dataset is not representative of all the possible sea/wind situations: there are only two samples where H_S is higher than 3 m and there are no samples with U higher than 12 ms^{-1}. Anyway, it can be seen that the trend is similar to the previous plots. The reader will notice that λ_C is on average lower than for S-1 dataset. This is because the range to platform ratio (R/V) is lower for CKS than for S-1 (see eq. 1).

5. CONCLUSIONS AND FUTURE WORKS

The azimuth wavelength cut-off (λ_C) approach for the wind speed (U) retrieval has been explored through a dataset of Sentinel-1 (S-1) multi-look SAR images. The analysis shows that λ_C has a linear dependency on U only when the sea state is fully developed. For such cases, a linear Geophysical Model Function (GMF) has been fitted and validated by comparing the retrieved values to a set of independent scatterometer measurements of the Chinese mission HY-2A.
The agreement is good especially for U higher than 15 ms^{-1}. For U lower than 15 ms^{-1} the retrieval is too noisy. The reasons should be further investigated and a more refined model that takes into account the directionality aspects of all the wave spectral components should be considered. In addition, the validation dataset should be expanded in order to include low wind/sea samples.
Furthermore, the new λ_C-GMF should be tested in conjunction with other GMFs in a Bayesian retrieval approach in order to evaluate its capability to produce additional fresh information. Finally, it would be interesting applying this λ_C-GMF to other SAR platforms and analyse the differences, given that the normalization for the acquisition geometry is produced.
In order to answer to the last question, a similar analysis has been produced for a dataset of X-band SAR images of the COSMO-SkyMed (CSK) mission. The trend of λ_C on U is similar, but the dataset should be largely expanded in order to account for all the possible sea/wind situations.

6. REFERENCES

1. Beal, R. C., D. G. Tilley, and F. M. Monaldo. 1983. "Large-and small-scale spatial evolution of digitally processed ocean wave spectra from SEASAT synthetic aperture radar." Journal of Geophysical Research: Oceans" 88 (C3): 1761-1778. http://dx.doi.org/10.1029/JC088iC03p01761.
2. Hasselmann, K., and S. Hasselmann. 1991. "On the nonlinear mapping of an ocean wave spectrum into a synthetic aperture radar image spectrum and its inversion." Journal of Geophysical Research: Oceans 96 (C6): 10713-10729. http://dx.doi.org/10.1029/91JC00302.
3. Hersbach, H., A. Sto_elen, and S. de Haan. 2007. "An improved C-band scatterometer ocean geophysical model function: CMOD5." Journal of Geophysical Research: Oceans 112 (C3) http://dx.doi.org/10.1029/2006JC003743.
4. Kerbaol V., Chapron B., Vachon P. W., 1998, "Analysis of ERS-1/2 synthetic aperture radar wave

mode imagettes", Journal of Geophysical Reserarch, Vol. 103, No. C4, pg 7833-7846

5. Mouche, A.A., F. Collard, B. Chapron, K. Dagestad, G. Guitton, J.A. Johannessen, V. Kerbaol, and M.W. Hansen. 2012. "On the Use of Doppler Shift for Sea Surface Wind Retrieval From SAR." Geoscience and Remote Sensing, IEEE Transactions on 50 (7): 290-2909.
6. Pierson, W. J., and L. Moskowitz. 1964. "A proposed spectral form for fully developed wind seas based on the similarity theory of S. A. Kitaigorodskii." Journal of Geophysical Research" 69 (24): 5181-5190. http://dx.doi.org/10.1029/JZ069i024p05181.
7. Vachon, P. W., H. E. Krogstad, and J. S. Paterson. 1994. "Airborne and spaceborne synthetic aperture radar observations of ocean waves." Atmosphere-Ocean 32 (1): 83-112. http://dx.doi.org/10.1080/07055900.1994.9649491.